Prepared for submission to JHEP

An alternative perspective to observe the critical phenomena of dilaton AdS black holes

arXiv:1607.03702v1 [gr-qc] 13 Jul 2016

Jie-Xiong Mo

Institute of Theoretical Physics, Lingnan Normal University, Zhanjiang, 524048, Guangdong, China

E-mail: mojiexiong@gmail.com

Abstract: The critical phenomena of dilaton AdS black holes are probed from a totally different perspective other than the $P-v$ criticality and the $q-U$ criticality discussed in the former literature. We investigate not only the two point correlation function but also the entanglement entropy of dilaton AdS black holes. We achieve this goal by solving the equation of motion constrained by the boundary condition numerically and we concentrate on δL and δS which have been regularized by subtracting the terms in pure AdS with the same boundary region. For both the two point correlation function and the entanglement entropy, we consider $4\times 2\times 2=16$ cases due to different choices of parameters. The van der Waals like behavior can be clearly witnessed from all the $T-\delta L$ $(T-\delta S)$ graphs for $q<q_c$. Moreover, the effects of dilaton gravity and the spacetime dimensionality on the phase structure of dilaton AdS black holes are disclosed. Furthermore, we discuss the stability of dilaton AdS black holes by applying the analogous specific heat definition and remove the unstable branch by introducing a bar $T=T_*$. It is shown that the first order phase transition temperature T_* is affected by both α and n. The analogous equal area laws for both the $T-\delta L$ graph and the $T-\delta S$ graph are examined numerically. The relative errors for all the cases are small enough that we can safely conclude that the analogous equal area laws hold for $T-\delta L$ $(T-\delta S)$ graph of dilaton AdS black holes.

Contents

1 Introduction **1**

2 A brief review of thermodynamics of dilaton AdS black holes **2**

3 Two point correlation function of dilaton AdS black holes and its van der Waals like behavior **3**

4 Numerical check of equal area law in $T - \delta L$ graph **4**

5 Entanglement entropy of dilaton AdS black holes and its van der Waals like behavior **6**

6 Numerical check of equal area law in $T - \delta S$ graph **11**

7 Conclusions **14**

1 Introduction

According to the well-known AdS/CFT correspondence [1–3], the physics in the bulk is related with the conformal field theory on the boundary one dimension fewer. Recently, Johnson disclosed intriguing properties of entanglement entropy [4] and further enhanced this relation. It was shown that the isocharges in the entanglement entropy-temperature plane and that of entropy-temperature plane not only enjoy similar behavior, but also share the same critical temperature and critical exponents [4]. Moreover, Ref. [5] proved that equal area law, which was shown to hold for $T - S$ curve in former literature[6], also holds for the entanglement entropy-temperature plane. Ref. [7] further showed that other nonlocal observable, such as two point correlation function, also display similar behavior as the entanglement entropy. The research topic initiated by Johnson is receiving more and more attention [8]-[15].

In this paper, we would like to generalize the above topic to dilaton AdS black holes to probe whether these phenomena are universal. On the other hand, our probe may be served as an alternative perspective to observe the critical phenomena of dilaton AdS black holes and would help deepen the understanding of these phenomena. Investigating the properties of AdS black holes in dilaton gravity is of interest itself. Dilaton field appears in the low energy limit of string theory and have significant impact on both the casual structure and thermodynamics of black holes. The action of dilaton gravity contains one or more Liouville-type potentials. These potentials are resulted by the breaking of spacetime supersymmetry in ten dimensions. Both the black hole solutions in dilaton gravity and their thermodynamics have attracted considerable attention [16]- [50].

The organization of this paper is as follows. Sec. 2 devotes to a brief review of thermodynamics of dilaton AdS black holes. In Sec. 3, we will study their two point correlation functions numerically while we will carry out numerical check of equal area law in Sec. 4. Furthermore, we will investigate their entanglement entropy numerically in Sec. 5 and check the corresponding equal area law in Sec. 6. The last section devotes to conclusions.

2 A brief review of thermodynamics of dilaton AdS black holes

The $(n+1)$-dimensional Einstein-Maxwell-Dilaton action reads [34–36]

$$S=\frac{1}{16\pi}\int d^{n+1}x\sqrt{-g}\left(R-\frac{4}{n-1}(\nabla\Phi)^2-V(\Phi)-(e^{-4\alpha\Phi/(n-1)}F_{\mu\nu}F^{\mu\nu}\right), \tag{2.1}$$

where Φ is the dilaton field with its potential denoted as $V(\Phi)$. R is the Ricci scalar curvature and $F_{\mu\nu}=\partial_\mu A_\nu-\partial_\nu A_\mu$ is the electromagnetic field tensor. The strength of coupling between the electromagnetic field and the scalar field is characterized by α.

The corresponding solution has been derived as [34–36]

$$ds^2 = -f(r)dt^2+\frac{1}{f(r)}dr^2+r^2R^2(r)d\Omega^2_{k,n-1}, \tag{2.2}$$

$$\Phi(r) = \frac{(n-1)\alpha}{2(\alpha^2+1)}\ln\left(\frac{b}{r}\right), \tag{2.3}$$

where

$$\begin{aligned} f(r) = &-\frac{k(n-2)(1+\alpha^2)^2b^{-2\gamma}r^{2\gamma}}{(\alpha^2-1)(\alpha^2+n-2)}-\frac{m}{r^{(n-1)(1-\gamma)-1}}\\ &-\frac{nb^{2\gamma}(1+\alpha^2)^2r^{2(1-\gamma)}}{l^2(\alpha^2-n)}+\frac{2q^2(1+\alpha^2)^2b^{-2(n-2)\gamma}r^{2(n-2)(\gamma-1)}}{(n-1)(n+\alpha^2-2)}, \end{aligned} \tag{2.4}$$

$$R(r) = e^{2\alpha\Phi(r)/(n-1)}. \tag{2.5}$$

k is a constant characterizing the hypersurface $d\Omega^2_{k,n-1}$ whose volume is denoted as ω_{n-1}. k can be taken as -1, 0, 1, corresponding to hyperbolic, flat and spherical constant curvature hypersurface respectively. γ is related to α by $\gamma=\alpha^2/(\alpha^2+1)$. b is an arbitrary constant while l is the AdS length scale. q and m are constants related to the charge Q and the mass M of the black hole as follows

$$M = \frac{b^{(n-1)\gamma}(n-1)\omega_{n-1}m}{16\pi(\alpha^2+1)}, \tag{2.6}$$

$$Q = \frac{\omega_{n-1}q}{4\pi}. \tag{2.7}$$

Based on both the fact that the term including m should vanish at spacial infinity and the fact that the electric potential A_t should be finite at infinity, Ref. [44] obtained the restrictions on α for dilaton black holes coupled with power-law Maxwell field as follow

$$\begin{aligned} &For\ \frac{1}{2}<p<\frac{n}{2},\quad 0\le\alpha^2<n-2,\\ &For\ \frac{n}{2}<p<n-1,\quad 2p-n<\alpha^2<n-2. \end{aligned} \tag{2.8}$$

Here, we consider the dilaton black holes coupled with standard Maxwell field in this paper, corresponding to the case $p = 1$. So the above restriction reduces to be $0 \leq \alpha^2 < n - 2$.

The Hawking temperature and the entropy have been derived as [36]

$$T = \frac{-(1+\alpha^2)}{2\pi(n-1)}\Big[\frac{k(n-2)(n-1)}{2b^{2\gamma}(\alpha^2-1)}r_+^{2\gamma-1} + \Lambda b^{2\gamma} r_+^{1-2\gamma} + q^2 b^{-2(n-2)\gamma} r_+^{(2n-3)(\gamma-1)-\gamma}\Big], \tag{2.9}$$

$$S = \frac{\omega_{n-1} b^{(n-1)\gamma} r_+^{(n-1)(1-\gamma)}}{4}, \tag{2.10}$$

where the relation $\Lambda = -n(n-1)/2l^2$ holds for $(n+1)$-dimensional AdS black holes.

Furthermore, Ref. [36] investigated the $P - v$ criticality of dilaton AdS black holes when Q was treated as an invariant parameter and the $q - U$ criticality (U denotes the electric potential) when l was treated as an invariant parameter. Both cases were shown to exhibit the van der Waals like behavior [36]. In the rest of this paper, we will further probe the critical phenomena of dilaton AdS black holes from an alternative perspective. Namely, the two point correlation function and the entanglement entropy.

3 Two point correlation function of dilaton AdS black holes and its van der Waals like behavior

Considering the points (t_0, x_i) and (t_0, x_j) on the AdS boundary with the corresponding bulk geodesic length denoted as L, the equal time two point correlation function in the large Δ limit (Δ denotes the conformal dimension of scalar operator $\mathcal{O}$ in the dual field theory) takes the following form [51]

$$\langle \mathcal{O}(t_0, x_i)\mathcal{O}(t_0, x_j)\rangle \approx e^{-\Delta L}. \tag{3.1}$$

The proper length can be obtained by parameterizing the trajectory with θ

$$L = \int_0^{\theta_0} \mathcal{L}(r(\theta), \theta) d\theta, \quad \mathcal{L} = \sqrt{\frac{r'^2}{f(r)} + r^2}, \tag{3.2}$$

where $r' = dr/d\theta$. Note that the boundary points have been chosen as $(\phi = \frac{\pi}{2}, \theta = 0)$ and $(\phi = \frac{\pi}{2}, \theta = \theta_0)$.

Applying the well-known Euler-Lagrange equation

$$\frac{\partial \mathcal{L}}{\partial r} = \frac{d}{d\theta}\left(\frac{\partial \mathcal{L}}{\partial r'}\right), \tag{3.3}$$

the equation of motion for $r(\theta)$ can be derived. Solving the equation of motion constrained by the boundary condition $r(0) = r_0, r'(0) = 0$, one can obtain $r(\theta)$ via numerical methods. To avoid the divergence, the geodesic length L_0 in pure AdS with the same boundary region should be subtracted from the geodesic length L, with the regularized geodesic length denoted as δL. Note that L_0 can also be obtained through numerical treatment.

To investigate the effect of dilaton gravity on the phase structure of two point correlation function, we focus on the cases that α is chosen as $0, 0.25, 0.5, 0.75$ respectively. Note

that we have considered the restriction $0 \leq \alpha^2 < n-2$ mentioned in the former section. The case $\alpha = 0$ is chosen so that one can compare the results with those of RN-AdS black holes.

On the other hand, n is chosen as $3, 4$ respectively to study the possible effect of space-time dimensionality. Moreover, we choose $\theta_0 = 0.2, 0.3$ to check whether different boundary region sizes exert influence on the phase structure just as shown in former literature [7]. In this paper the cutoff θ_c will be chosen as $0.199, 0.299$ accordingly and the AdS radius l will be set to be one.

To summarize, we consider $4 \times 2 \times 2 = 16$ cases due to different choices of parameters. In each case we concentrate on the case $q < q_c$ (q_c denotes the critical value of the parameter q) to probe the possible van der Waals behavior in the $T - \delta L$ graphs. Fig. 1(a)-1(d) show respectively the cases of $n = 3, \theta_0 = 0.2$ with four different choices of α while Fig. 2(a)-2(d) display the cases for $n = 4, \theta_0 = 0.2$. The cases for $n = 3, \theta_0 = 0.3$ are depicted in Fig. 3(a)-3(d) while the cases for $n = 4, \theta_0 = 0.3$ are depicted in Fig. 4(a)-4(d).

From all the $T - \delta L$ graphs for $q < q_c$, the van der Waals like behavior can be clearly witnessed. There exist both the local maximum temperature and the local minimum temperature, which we denote as T_{max} and T_{min} respectively. As shown in Fig. 1-Fig. 4, the effects of dilaton gravity are reflected in two ways. Firstly, as the increasing of the parameter α, T_{max} and T_{min} both increase. Secondly, the corresponding δL also increase when α increases. And this phenomena is more apparent for large α. Comparing Fig. 1 with Fig. 2, one may find that the case $n = 4$ has higher T_{max} and T_{min} than the case $n = 3$. This can also be witnessed by comparing Fig. 3 with Fig. 4. On the other hand, the effect of boundary region size is quite apparent in the range of δL axis when one compares Fig. 1 with Fig. 3, or compares Fig. 2 with Fig. 4.

4 Numerical check of equal area law in $T - \delta L$ graph

According to the analogous specific heat for $T - \delta L$ graph introduced in Ref. [7]

$$C = T\frac{\partial \delta L}{\partial T}, \tag{4.1}$$

$T - \delta L$ graph for $q < q_c$ can be divided into three branches. Namely, the stable large radius branch with positive specific heat, the unstable medium radius branch with negative specific heat and the stable small radius branch with positive specific heat. This phenomena is quite similar to that of $T - S$ graph and $P - v$ graph of dilaton AdS black holes.

One can remove the unstable branch in $T - \delta L$ curve with a bar $T = T_*$ vertical to the temperature axis by mimicking the approach of $T - S$ graph [6]. Note that T_* should be interpreted physically as the first order phase transition temperature and can be determined utilizing the free energy analysis. The analogous equal area law for the $T - \delta L$ graph reads

$$T_* \times (\delta L_3 - \delta L_1) = \int_{\delta L_1}^{\delta L_3} T d\delta L, \tag{4.2}$$

where δL_1, δL_2, δL_3 are three values of δL corresponding to T_*. Here, we have assumed that $\delta L_1 < \delta L_2 < \delta L_3$. If one can prove that the L. H. S of Eq. 4.2 equal to its R. H. S,

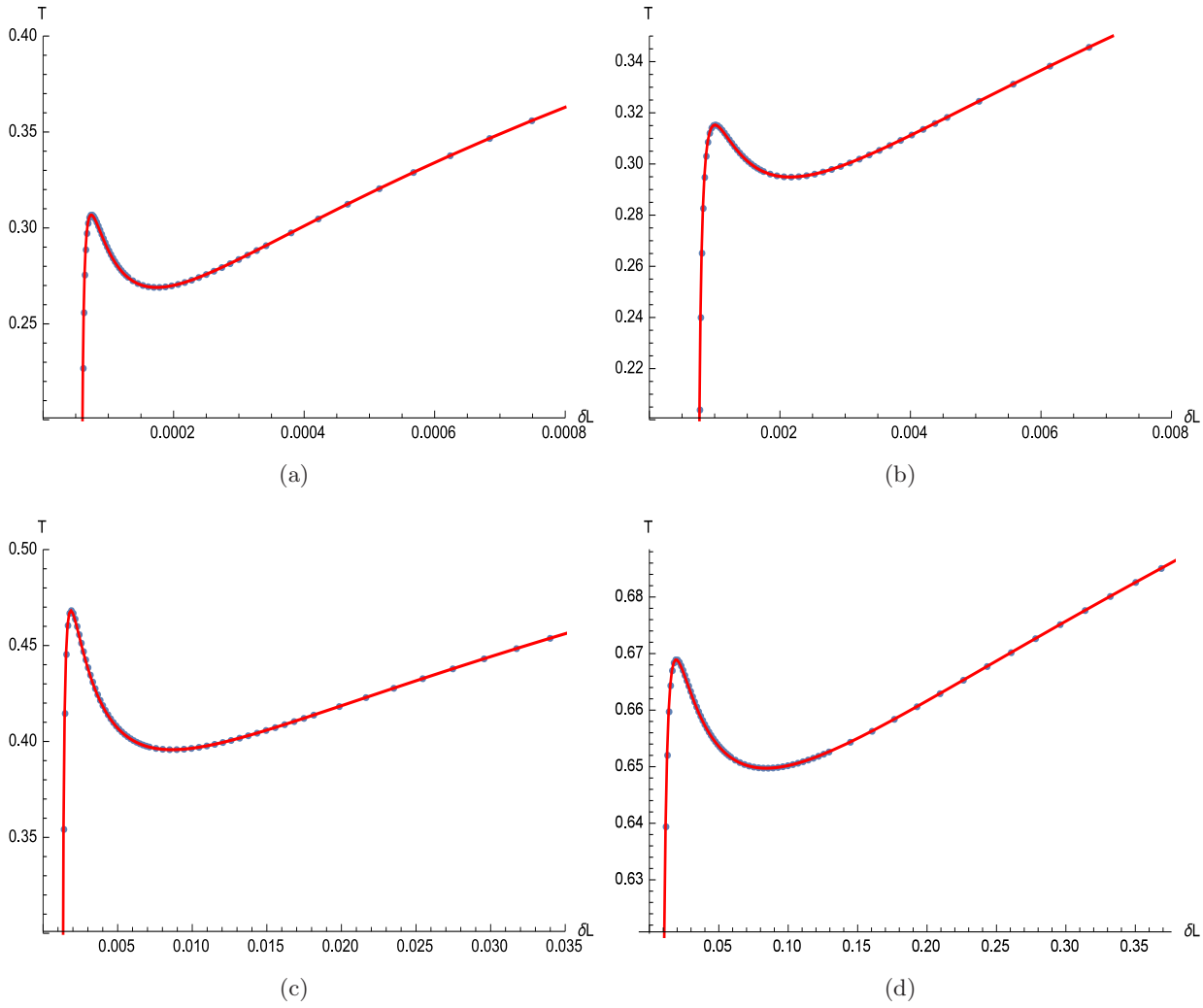

Figure 1. T vs. δL for $n = 3, \theta_0 = 0.2$ (a) $\alpha = 0, q = 0.12$ (b) $\alpha = 0.25, q = 0.12$ (c) $\alpha = 0.5, q = 0.06$ (d) $\alpha = 0.75, q = 0.06$

one can draw the conclusion that the analogous equal area law holds for the $T - \delta L$ graph of dilaton AdS black holes.

Before we carry out the examination, it is urgent to study the behavior of free energy first. Utilizing Eqs. 2.4, 2.6, 2.9 and 2.10, the free energy of dilaton AdS black holes can be derived as

$$F = M - TS = \frac{\omega_{n-1}(1+\alpha^2)b^{(n-1)\gamma}r_+^{n-2+\gamma-n\gamma}}{16\pi} \times \Big\{\frac{k(n-2)r_+^{2\gamma}b^{-2\gamma}}{n-2+\alpha^2} + \frac{nb^{2\gamma}r_+^{2-2\gamma}(\alpha^2-1)}{l^2(n-\alpha^2)} + \frac{2b^{-2(n-2)\gamma}q^2 r_+^{2(n-2)(\gamma-1)}(2n-3+\alpha^2)}{(n-1)(n-2+\alpha^2)}\Big\}, \tag{4.3}$$

with the $F - T$ graphs depicted in Fig. 5 and Fig. 6 for different choices of parameters.

One can observe the familiar swallow tail behavior in all the $F - T$ graphs and obtain T_* from the intersection point of two branches in the graphs. Comparing these graphs,

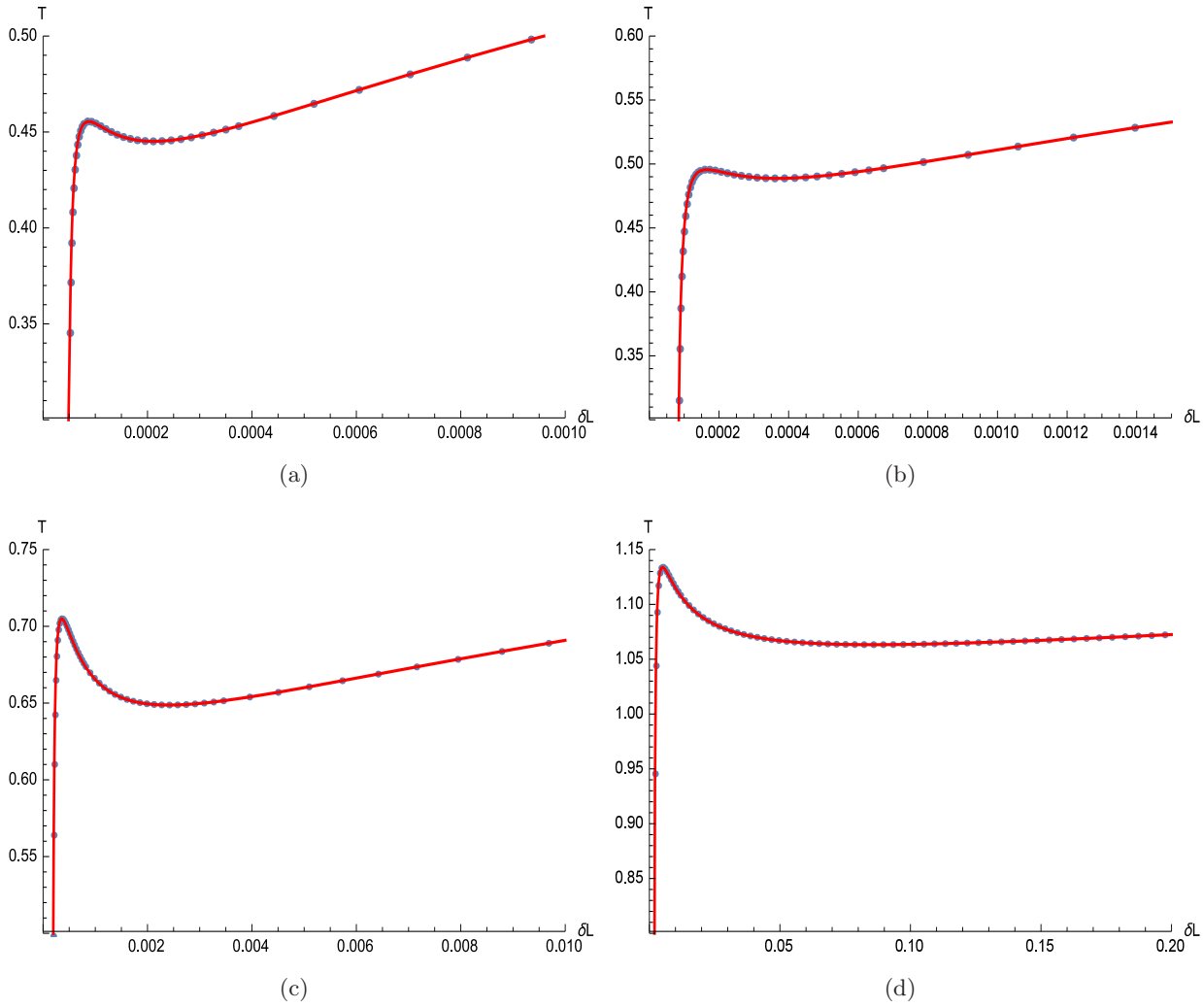

Figure 2. T vs. δL for $n = 4, \theta_0 = 0.2$ (a) $\alpha = 0, q = 0.12$ (b) $\alpha = 0.25, q = 0.12$ (c) $\alpha = 0.5, q = 0.06$ (d) $\alpha = 0.75, q = 0.06$

one may conclude that the first order phase transition temperature T_* is affected by both α and n. When α increases, T_* increases. When n increases, T_* increases too. With T_* at hand, one can calculate the left-hand side and right-hand side of Eq.(4.2) for different cases. As can be seen from Table 1-Table 4, the relative errors for all the cases are small enough and we can safely conclude that the analogous equal area law holds for $T - \delta L$ graph of dilaton AdS black holes.

5 Entanglement entropy of dilaton AdS black holes and its van der Waals like behavior

Besides the two point correlation function, entanglement entropy serves as another nonlocal observable to probe the holographic properties of black holes.

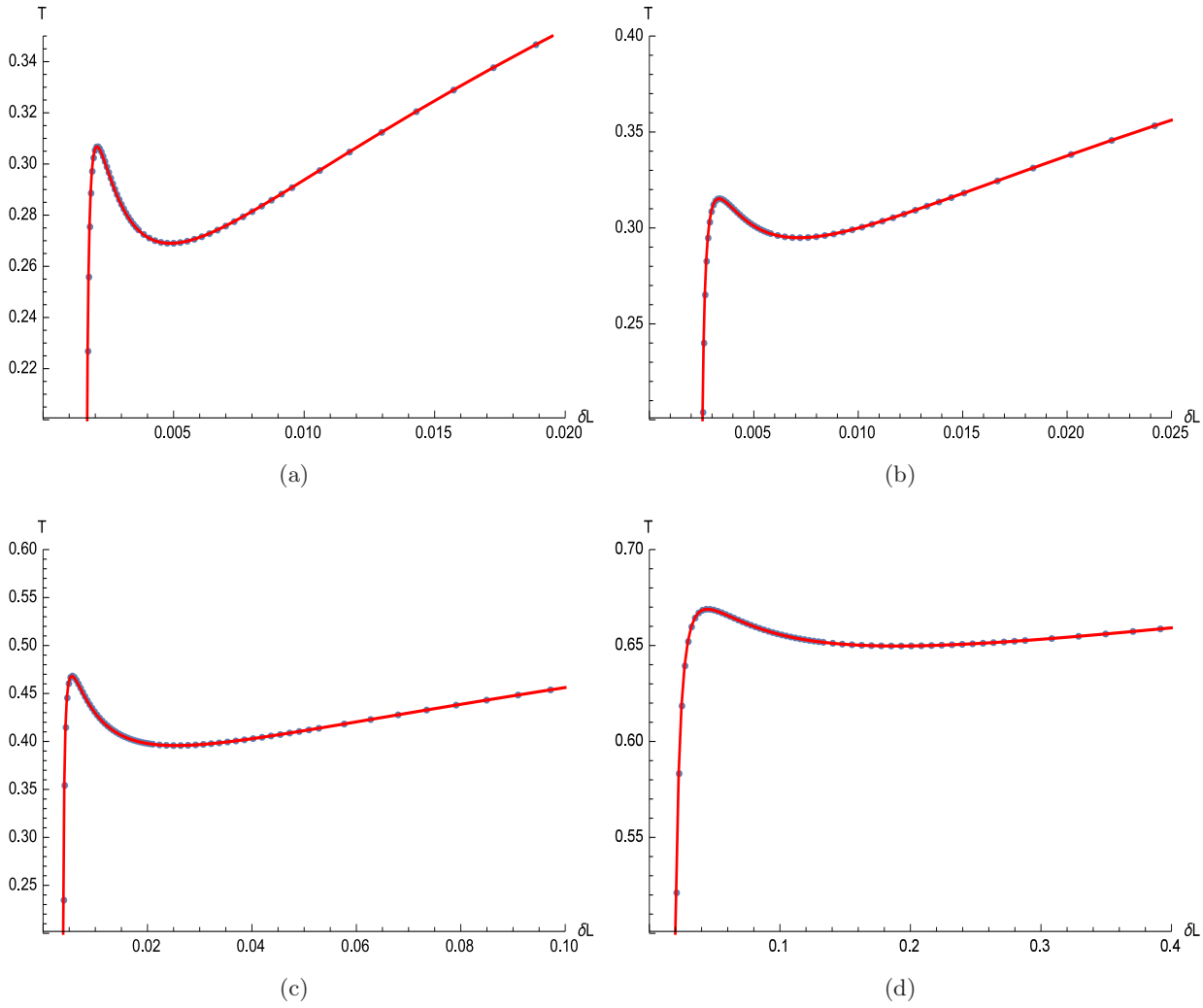

Figure 3. T vs. δL for $n = 3, \theta_0 = 0.3$ (a) $\alpha = 0, q = 0.12$ (b) $\alpha = 0.25, q = 0.12$ (c) $\alpha = 0.5, q = 0.06$ (d) $\alpha = 0.75, q = 0.06$

Table 1. Numerical check of equal area law in $T - \delta L$ graph for $n = 3, \theta_0 = 0.2, l = 1, b = 1, k = 1$

α	q	T_*	δL_1	δL_3	$T_*(\delta L_3 - \delta L_1)$	$\int_{\delta L_1}^{\delta L_3} T d\delta L$	relative error
0	0.12	0.277496	0.0000637680	0.0002613560	0.0000548299	0.0000549115	0.1486%
0.25	0.12	0.3002889	0.0007501943	0.0030534139	0.0006916313	0.0006854523	0.9014%
0.50	0.06	0.4078042	0.0014369702	0.0157774345	0.0058481016	0.0058594007	0.1928%
0.75	0.06	0.65401625	0.0130252955	0.1416948822	0.0841520006	0.0841644278	0.0148%

The entanglement entropy can be expressed holographically in terms of the area of a minimal surface anchored on ∂A as [52, 53]

$$S_A = \frac{Area(\Sigma)}{4G_N}, \tag{5.1}$$

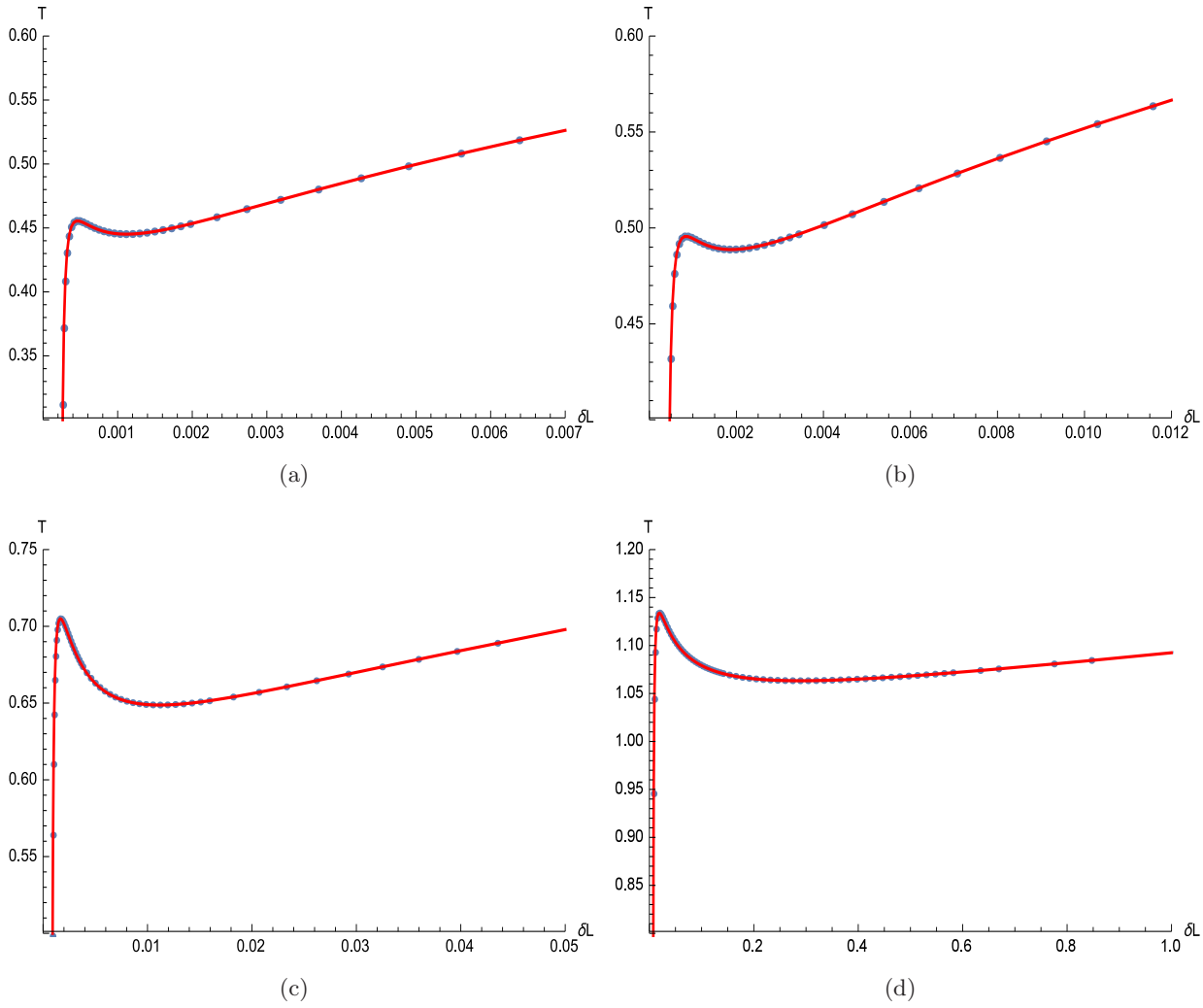

Figure 4. T vs. δL for $n = 4, \theta_0 = 0.3$ (a) $\alpha = 0, q = 0.12$ (b) $\alpha = 0.25, q = 0.12$ (c) $\alpha = 0.5, q = 0.06$ (d) $\alpha = 0.75, q = 0.06$

Table 2. Numerical check of equal area law in $T - \delta L$ graph for $n = 4, \theta_0 = 0.2, l = 1, b = 1, k = 1$

α	q	T_*	δL_1	δL_3	$T_*(\delta L_3 - \delta L_1)$	$\int_{\delta L_1}^{\delta L_3} T d\delta L$	relative error
0	0.12	0.448178	0.0000688919	0.0003011692	0.0001041016	0.0001041083	0.0064%
0.25	0.12	0.490898	0.0001308121	0.0005050468	0.0001837111	0.0001837165	0.0029%
0.50	0.06	0.65793667	0.0002371822	0.0046525001	0.0029049996	0.0029063836	0.0476%
0.75	0.06	1.070886315	0.0027446929	0.1854763902	0.1956848740	0.1957787303	0.0479%

where Σ is the codimension-2 minimal surface with boundary condition $\partial\Sigma = \partial A$ and G_N is the Newton's constant.

As argued in Ref. [5], one can avoid dealing with the phase transition between connected and disconnected minimal surfaces by avoiding large entangling regions. For this

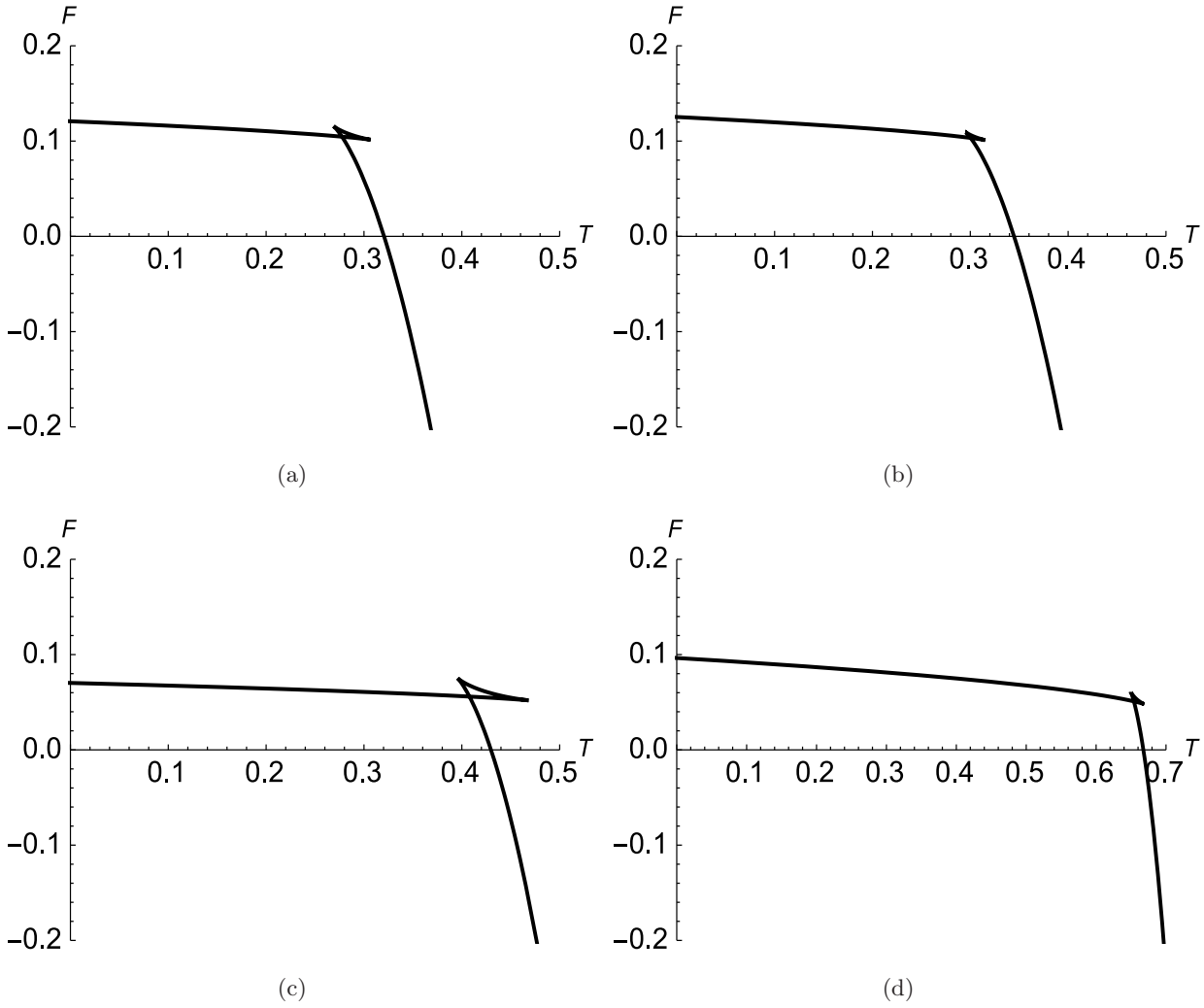

Figure 5. F vs. T for $n = 3, l = 1, b = 1, k = 1$ (a) $\alpha = 0, q = 0.12$ (b) $\alpha = 0.25, q = 0.12$ (c) $\alpha = 0.50, q = 0.06$ (d) $\alpha = 0.75, q = 0.06$

Table 3. Numerical check of equal area law in $T - \delta L$ graph for $n = 3, \theta_0 = 0.3, l = 1, b = 1, k = 1$

α	q	T_*	δL_1	δL_3	$T_*(\delta L_3 - \delta L_1)$	$\int_{\delta L_1}^{\delta L_3} T d\delta L$	relative error
0	0.12	0.277496	0.0017837032	0.0073122615	0.0015341528	0.0015366458	0.1622%
0.25	0.12	0.3002889	0.0024892165	0.0101203310	0.0022915390	0.0022710854	0.9006%
0.50	0.06	0.4078042	0.0042562477	0.0460392623	0.0170392888	0.0170769726	0.2207%
0.75	0.06	0.65401625	0.0301340104	0.3145252201	0.1859964725	0.1860497056	0.0286%

consideration, we choose the region to be a spherical cap on the boundary delimited by $\theta \leq \theta_0$.

Parametrizing the minimal surface by the function $r(\theta)$, the holographic entanglement

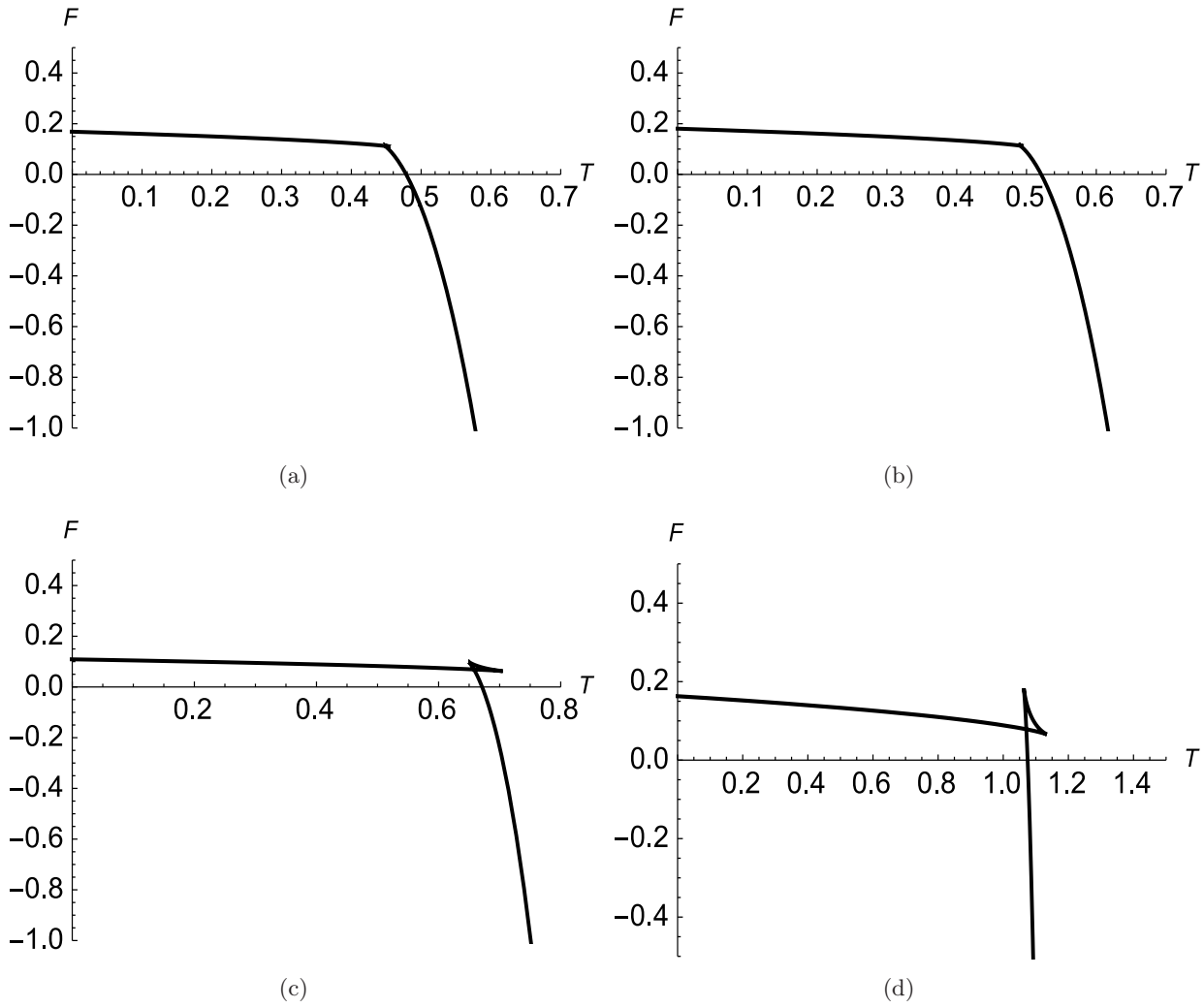

Figure 6. F vs. T for $n = 4, l = 1, b = 1, k = 1$ (a) $\alpha = 0, q = 0.12$ (b) $\alpha = 0.25, q = 0.12$ (c) $\alpha = 0.50, q = 0.06$ (d) $\alpha = 0.75, q = 0.06$

Table 4. Numerical check of equal area law in $T - \delta L$ graph for $n = 4, \theta_0 = 0.3, l = 1, b = 1, k = 1$

α	q	T_*	δL_1	δL_3	$T_*(\delta L_3 - \delta L_1)$	$\int_{\delta L_1}^{\delta L_3} T d\delta L$	relative error
0	0.12	0.448178	0.0003666396	0.0015882967	0.0005475198	0.0005475520	0.0059%
0.25	0.12	0.490898	0.0006709414	0.0025817161	0.0009379955	0.0009380156	0.0021%
0.50	0.06	0.65793667	0.0011076791	0.0213463021	0.0133157322	0.0133239547	0.0617%
0.75	0.06	1.070886315	0.0104051412	0.5641278672	0.5929740896	0.5938277878	0.1438%

entropy can be obtained as

$$S_A = \frac{\pi}{2} \int_0^{\theta_0} r \sin\theta \sqrt{\frac{r'^2}{f(r)} + r^2} d\theta, \tag{5.2}$$

where $r' = dr/d\theta$. From the above equation, one can obtain

$$\mathcal{L} = r\sin\theta\sqrt{\frac{r'^2}{f(r)} + r^2}. \tag{5.3}$$

Substituting it into Euler-Lagrange equation, one can derive the equation for $r(\theta)$. Then one can obtain $r(\theta)$ by solving the equation constrained by the boundary condition $r(0) = r_0, r'(0) = 0$ numerically.

To avoid the divergence, the holographic entanglement entropy should be regularized by subtracting the entanglement entropy S_0 (S_0 can also be obtained through numerical treatment) in pure AdS with the same boundary region. We denote the regularized entanglement entropy as δS and mainly deal with the behavior of $T - \delta S$ graph in the following discussions.

As in Sec. 3, we will consider $4 \times 2 \times 2 = 16$ cases due to different choices of parameters. For the sake of clarity, we repeat the choices here. α is chosen as $0, 0.25, 0.5, 0.75$ respectively to investigate the effect of dilaton gravity on the phase structure of holographic entanglement entropy while n is chosen as $3, 4$ respectively to probe the effect of spacetime dimensionality. θ_0 is chosen as $0.2, 0.3$ respectively to study the effect of different boundary region sizes. And the cutoff θ_c will also be chosen as $0.199, 0.299$ accordingly. In each case we focus on the case $q < q_c$ to probe the possible van der Waals behavior.

We plot the cases of $n = 3, \theta_0 = 0.2$ in Fig. 7(a)-7(d) and the cases of $n = 4, \theta_0 = 0.2$ in Fig. 8(a)-8(d). The cases for $n = 3, \theta_0 = 0.3$ are displayed in Fig. 9(a)-9(d) while the cases for $n = 4, \theta_0 = 0.3$ are depicted in Fig. 10(a)-10(d).

The van der Waals like behavior can be clearly witnessed from all the $T - \delta S$ graphs for $q < q_c$. As the $T - \delta L$ graphs presented in Sec. 3, there also exist both the local maximum temperature and the local minimum temperature in all the $T - \delta S$ graphs. As depicted in Fig. 7-Fig. 10, not only T_{max} and T_{min} but also the corresponding δS increase as the increasing of the parameter α, showing the impact of dilaton gravity. Comparing Fig. 7 with Fig. 8, or comparing Fig. 9 with Fig. 10, it is not difficult to observe that the cases $n = 4$ have higher T_{max} and T_{min} than the cases $n = 3$. Moreover, the range of δS axis for the cases $\theta_0 = 0.2$ differs from that of the cases $\theta_0 = 0.3$, showing the effect of boundary region size. These phenomena are quite similar to those of two point correlation function probed in Sec. 3.

6 Numerical check of equal area law in $T - \delta S$ graph

The analogous specific heat for $T - \delta S$ graph has been defined in former literature [7] as

$$C = T\frac{\partial \delta S}{\partial T}. \tag{6.1}$$

Based on the above definition, one can divide each $T - \delta S$ graph for $q < q_c$ into three branches. Namely, the stable large radius branch with positive specific heat, the unstable medium radius branch with negative specific heat and the stable small radius branch with positive specific heat. This phenomena is quite similar to that of $T - S$ graph and $P - v$

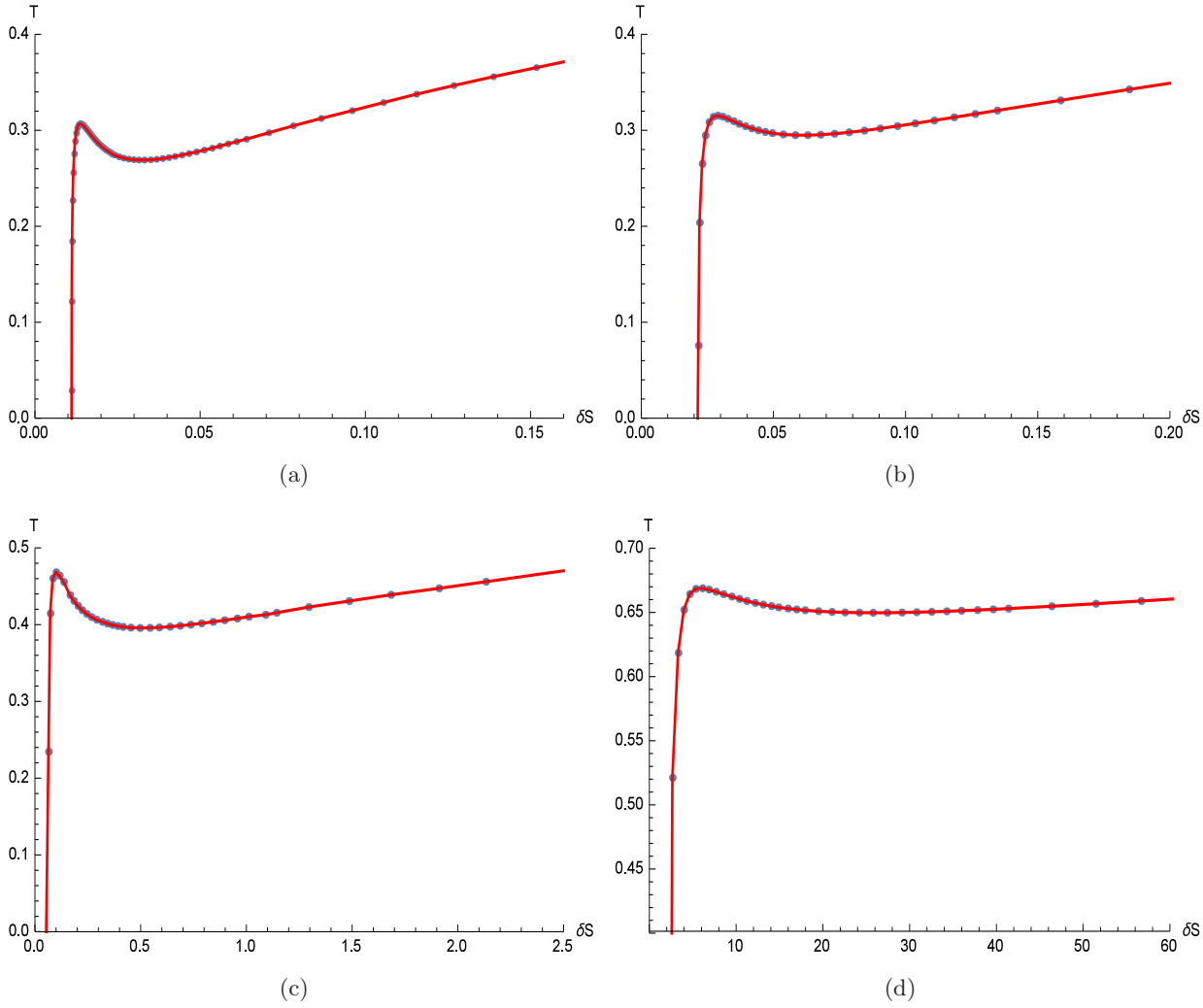

Figure 7. T vs. δS for $n = 3, \theta_0 = 0.2$ (a) $\alpha = 0, q = 0.12$ (b) $\alpha = 0.25, q = 0.12$ (c) $\alpha = 0.5, q = 0.06$ (d) $\alpha = 0.75, q = 0.06$

graph of dilaton AdS black holes. It is also similar to that of $T - \delta L$ graph discussed in Sec. 3.

Taking a similar treatment, one can remove the unstable branch in $T - \delta S$ curve with a bar $T = T_*$ vertical to the temperature axis. And the analogous equal area law for the $T - \delta S$ graph can be written as

$$T_* \times (\delta S_3 - \delta S_1) = \int_{\delta S_1}^{\delta S_3} T d\delta S, \tag{6.2}$$

where δS_1, δS_2, δS_3 are three values of δS corresponding to T_* with the assumption that $\delta S_1 < \delta S_2 < \delta S_3$.

We calculate the left-hand side and right-hand side of Eq.(6.2) for different cases and list the results in Table 5- Table 8, from which one can see clearly that the relative errors for

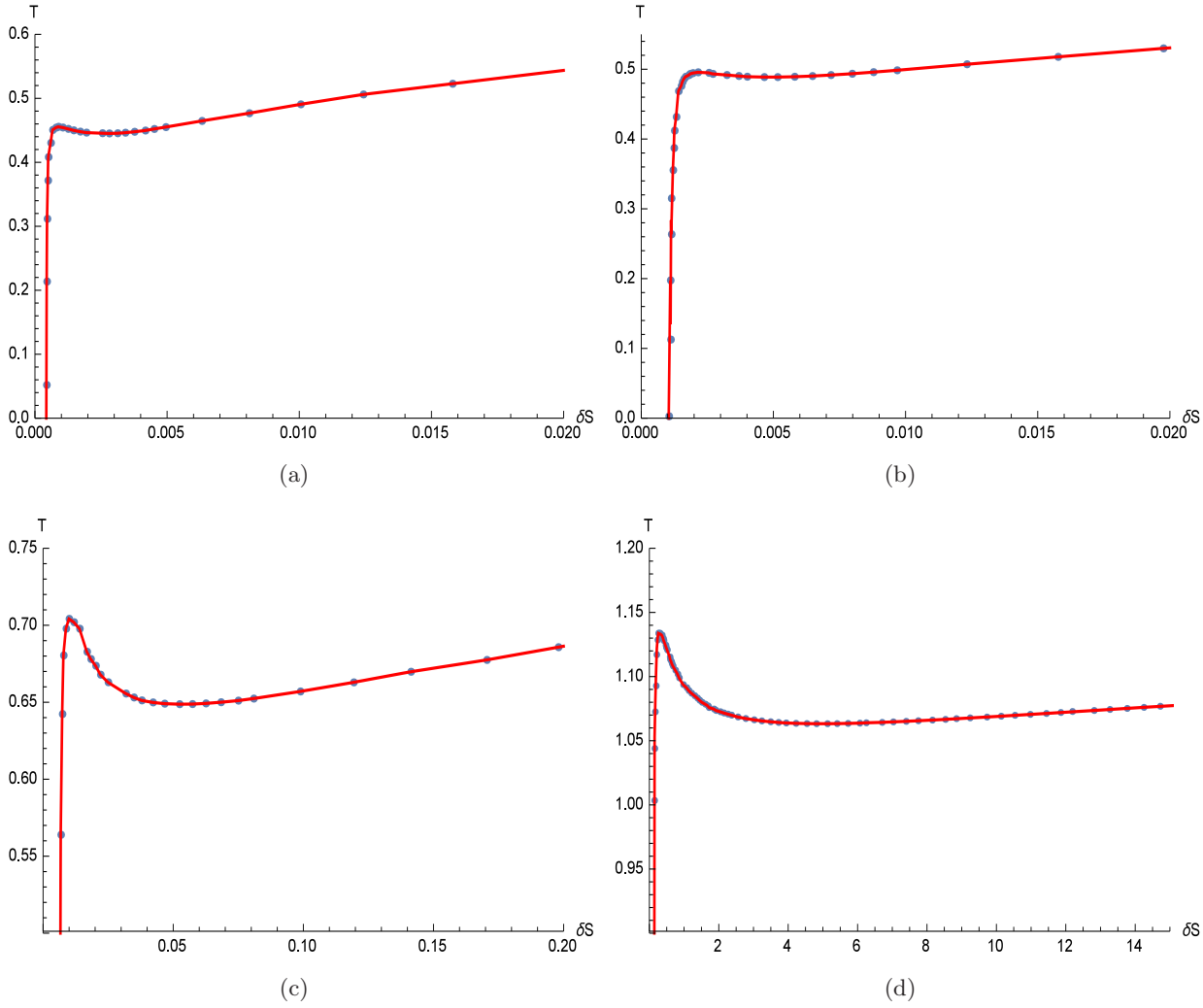

Figure 8. T vs. δS for $n = 4, \theta_0 = 0.2$ (a) $\alpha = 0, q = 0.12$ (b) $\alpha = 0.25, q = 0.12$ (c) $\alpha = 0.5, q = 0.06$ (d) $\alpha = 0.75, q = 0.06$

all the cases are amazingly small. So we can safely draw the conclusion that the analogous equal area law Eq.(6.2) holds for $T - \delta S$ graph of dilaton AdS black holes.

Table 5. Numerical check of equal area law in $T - \delta S$ graph for $n = 3, \theta_0 = 0.2, l = 1, b = 1, k = 1$

α	q	T_*	δS_1	δS_3	$T_*(\delta S_3 - \delta S_1)$	$\int_{\delta S_1}^{\delta S_3} T d\delta S$	relative error
0	0.12	0.277496	0.0119147123	0.0488420932	0.0102472005	0.0102600904	0.1256%
0.25	0.12	0.3002889	0.0247660099	0.0858928910	0.0183557239	0.0183641401	0.0458%
0.50	0.06	0.4078042	0.0716592283	0.9511787777	0.3586717662	0.3592798682	0.1693%
0.75	0.06	0.65401625	4.0720587420	44.1845284093	26.2342069900	26.2343780610	0.0007%

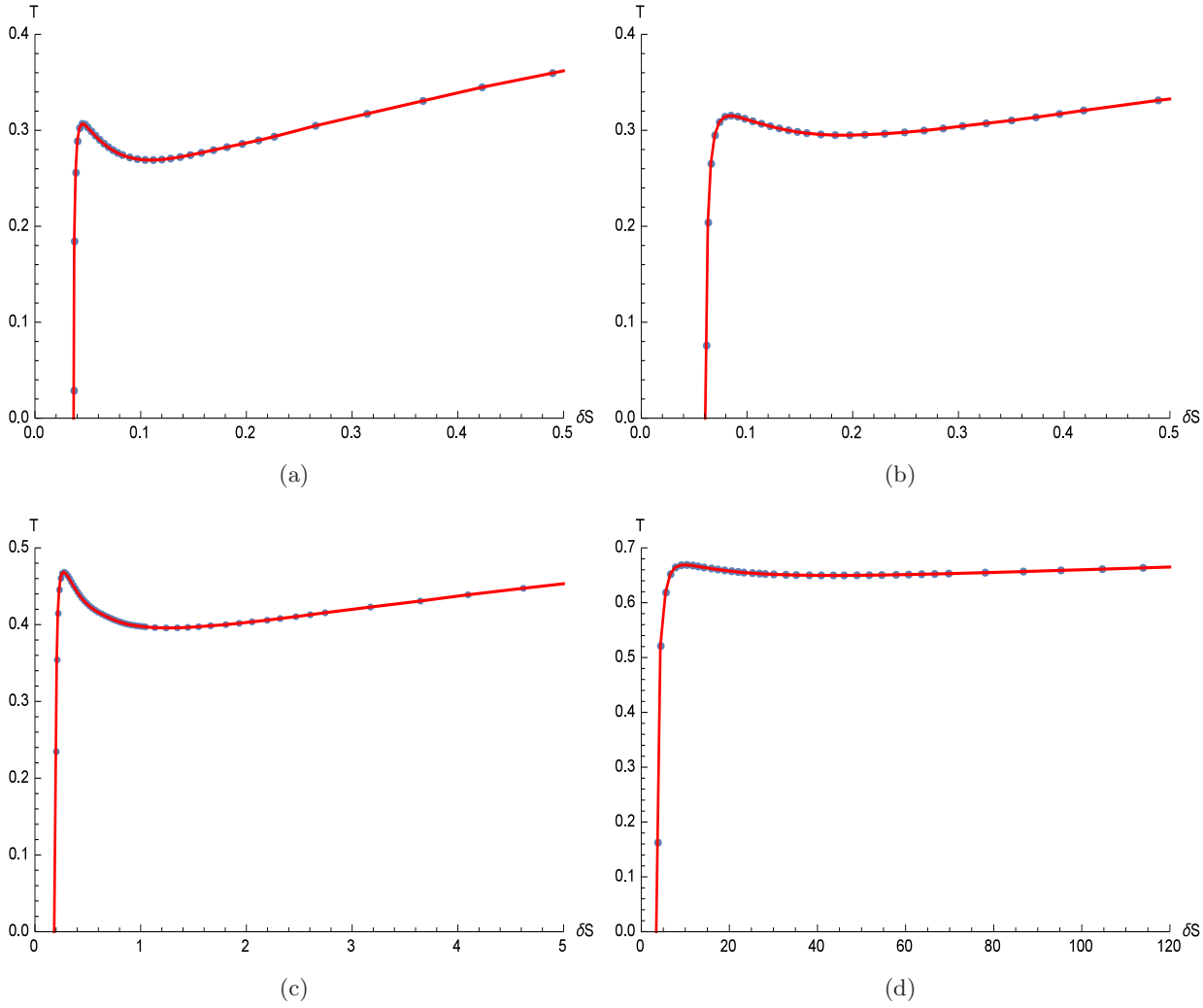

Figure 9. T vs. δS for $n = 3, \theta_0 = 0.3$ (a) $\alpha = 0, q = 0.12$ (b) $\alpha = 0.25, q = 0.12$ (c) $\alpha = 0.5, q = 0.06$ (d) $\alpha = 0.75, q = 0.06$

Table 6. Numerical check of equal area law in $T - \delta S$ graph for $n = 4, \theta_0 = 0.2, l = 1, b = 1, k = 1$

α	q	T_*	δS_1	δS_3	$T_*(\delta S_3 - \delta S_1)$	$\int_{\delta S_1}^{\delta S_3} T d\delta S$	relative error
0	0.12	0.448178	0.0006548237	0.0038527782	0.0014332529	0.0014330141	0.0167%
0.25	0.12	0.490898	0.0017571468	0.0067818433	0.0024666135	0.0024663505	0.0107%
0.50	0.06	0.65793667	0.0075207833	0.1020304981	0.0621814070	0.0622185738	0.0597%
0.75	0.06	1.070886315	0.1595664149	11.1997305875	11.8227607278	11.8253260328	0.0217%

7 Conclusions

In this paper, we probe the critical phenomena of dilaton AdS black holes from a totally different perspective other than the $P - v$ criticality and the $q - U$ criticality discussed in

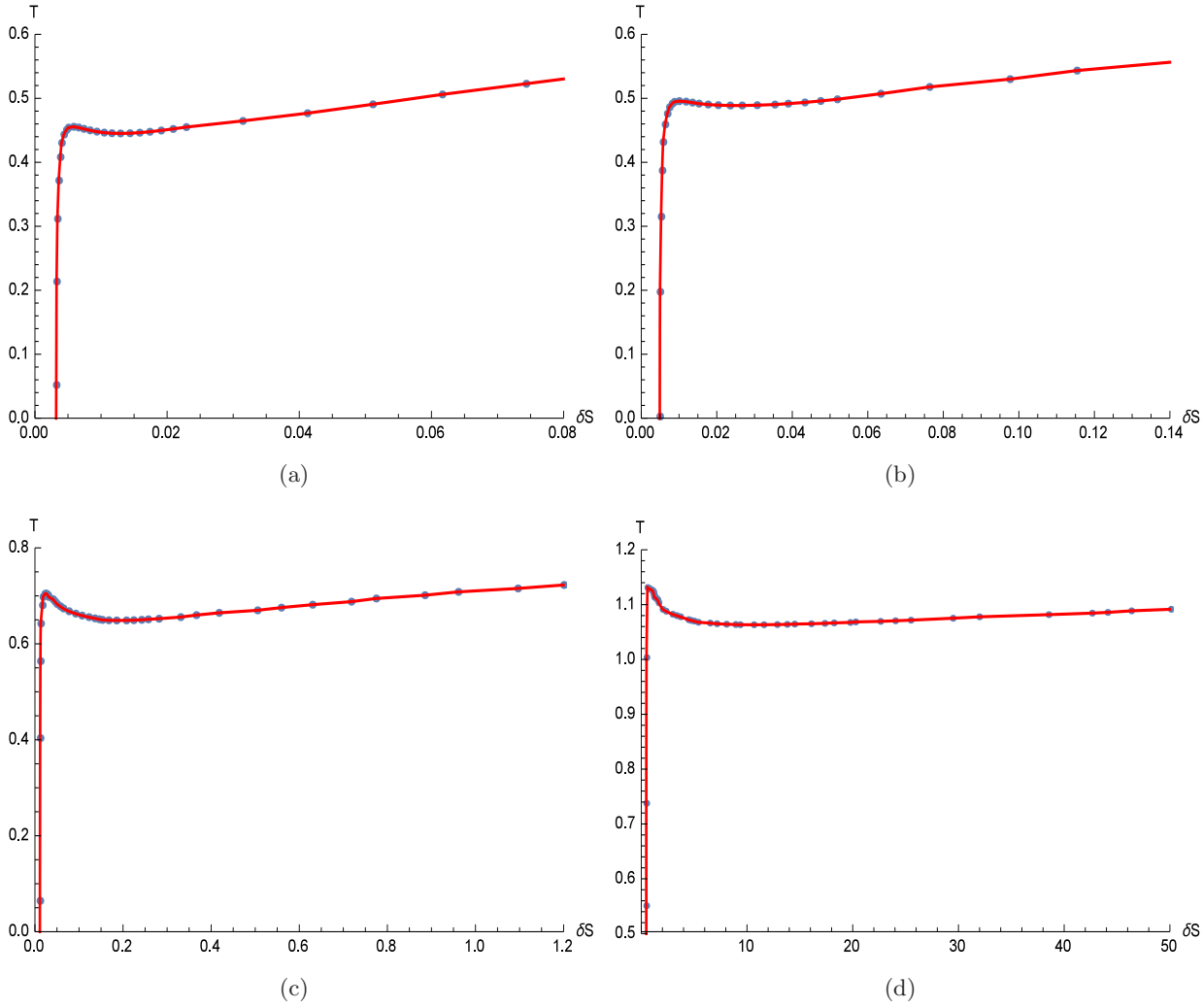

Figure 10. T vs. δS for $n = 4, \theta_0 = 0.3$ (a) $\alpha = 0, q = 0.12$ (b) $\alpha = 0.25, q = 0.12$ (c) $\alpha = 0.5, q = 0.06$ (d) $\alpha = 0.75, q = 0.06$

Table 7. Numerical check of equal area law in $T - \delta S$ graph for $n = 3, \theta_0 = 0.3, l = 1, b = 1, k = 1$

α	q	T_*	δS_1	δS_3	$T_*(\delta S_3 - \delta S_1)$	$\int_{\delta S_1}^{\delta S_3} T d\delta S$	relative error
0	0.12	0.277496	0.0394539472	0.1608172794	0.0336778392	0.0337657232	0.2603%
0.25	0.12	0.3002889	0.0711468332	0.2719042091	0.0602852116	0.0603586328	0.1216%
0.50	0.06	0.4078042	0.2149538454	2.3059365730	0.8527115384	0.8534806310	0.0901%
0.75	0.06	0.65401625	6.7549216837	74.3949477659	44.2376762082	44.2373479097	0.0007%

the former literature [36].

On the one hand, we study the two point correlation function of dilaton AdS black holes. Considering the points (t_0, x_i) and (t_0, x_j) on the AdS boundary, one can write the equal time two point correlation function in the large Δ limit and obtain the proper

Table 8. Numerical check of equal area law in $T-\delta S$ graph for $n=4, \theta_0=0.3, l=1, b=1, k=1$

α	q	T_*	δS_1	δS_3	$T_*(\delta S_3-\delta S_1)$	$\int_{\delta S_1}^{\delta S_3} T d\delta S$	relative error
0	0.12	0.448178	0.0046156698	0.0177350761	0.0058798293	0.0058821069	0.0387%
0.25	0.12	0.490898	0.0080413189	0.0369024703	0.0141678815	0.0141621430	0.0405%
0.50	0.06	0.65793667	0.0145412501	0.3493654246	0.2202931024	0.2207464643	0.2054%
0.75	0.06	1.070886315	0.5398143877	24.4969431344	25.6553613215	25.6488620105	0.0253%

length by parameterizing the trajectory with θ. Applying the Euler-Lagrange equation, one can derive the equation of motion for $r(\theta)$. Solving this equation constrained by the boundary condition $r(0)=r_0, r'(0)=0$, we obtain $r(\theta)$ via numerical methods. To avoid the divergence, we regularize the geodesic length by subtracting the geodesic length L_0 in pure AdS with the same boundary region.

On the other hand, we investigate the entanglement entropy of dilaton AdS black holes which can be expressed holographically in terms of the area of a minimal surface Σ anchored on ∂A with boundary condition $\partial\Sigma=\partial A$. We choose the region to be a spherical cap on the boundary delimited by $\theta\leq\theta_0$ and obtain the holographic entanglement entropy through parametrizing the minimal surface by $r(\theta)$, Utilizing the Euler-Lagrange equation again, we derive the equation for $r(\theta)$. Solving the equation constrained by the boundary condition numerically, we obtain $r(\theta)$. For similar consideration, we regularize the entanglement entropy by subtracting the entanglement entropy S_0 in pure AdS with the same boundary region.

For both the two point correlation function and the entanglement entropy, we consider $4\times2\times2=16$ cases due to different choices of parameters. Namely, α is chosen as $0, 0.25, 0.5, 0.75$ respectively to probe the effect of dilaton gravity on the phase structure while n is chosen as $3, 4$ respectively to study the impact of spacetime dimensionality. θ_0 is chosen as $0.2, 0.3$ respectively to check the effect of different boundary region sizes. The behavior of $T-\delta L$ graphs is quite similar to that of $T-\delta S$ graphs. Firstly, the van der Waals like behavior can be clearly witnessed from all the $T-\delta L$ ($T-\delta S$) graphs for $q<q_c$. Secondly, there exist both the local maximum temperature and the local minimum temperature. Thirdly, not only T_{max} and T_{min} but also the corresponding δL (δS) increase as the increasing of the parameter α, showing the impact of dilaton gravity. This phenomena is more apparent for large α. Fourthly, T_{max} and T_{min} of the cases $n=4$ is higher than that of the cases $n=3$. Lastly, the effect of boundary region size is quite apparent in the range of δL (δS) axis.

Furthermore, we discuss the stability of dilaton AdS black holes by introducing the analogous specific heat for $T-\delta L$ graph and $T-\delta S$ graph accordingly. All these graphs can be divided into three branches. Namely, the stable large radius branch with positive specific heat, the unstable medium radius branch with negative specific heat and the stable small radius branch with positive specific heat. This phenomena is quite similar to that of $T-S$ graph and $P-v$ graph of dilaton AdS black holes in former research. To remove

the unstable branch, we introduce a bar $T = T_*$ vertical to the temperature axis. T_* should be interpreted physically as the first order phase transition temperature and can be determined utilizing the free energy analysis. It is shown that the first order phase transition temperature T_* is affected by both α and n. When α increases, T_* increases. When n increases, T_* increases too. We also examine the analogous equal area law for both the $T - \delta L$ graph and the $T - \delta S$ graph respectively. The relative errors for all the cases are small enough that we can safely conclude that the analogous equal area law holds for $T - \delta L$ ($T - \delta S$) graph of dilaton AdS black holes.

Acknowledgments

The author would like to express his sincere gratitude to Dr. Jieci Wang, Dr. Xiongjun Fang, Dr. Zixu Zhao, Prof. Jia-Lin Zhang, Prof. Qiyuan Pan, Prof. Songbai Chen and Prof. Jiliang Jing for their warm hospitality during the Summer School and Workshop on Gravitation and Cosmology held in Hunan Normal University. The author also want to thank Dr. Xiao-Xiong Zeng for helpful discussions on numerics.

References

[1] J. M. Maldacena, Large N limit of superconformal field theories and supergravity, Int. J. Theor. Phys. 38, 1113 (1999)

[2] E. Witten, Anti-de Sitter space and holography, Adv. Theor. Math. Phys. 2, 253(1998)

[3] S. S. Gubser, I. R. Klebanov, A. M. Polyakov, Gauge theory correlators from noncritical string theory, Phys. Lett. B 428, 105 (1998)

[4] C. V. Johnson, Large N Phase Transitions, Finite Volume, and Entanglement Entropy, JHEP 1403 (2014) 047

[5] P. H. Nguyen, An equal area law for holographic entanglement entropy of the AdS-RN black hole, JHEP 1512 (2015) 139

[6] E. Spallucci and A. Smailagic, Maxwell's equal area law for charged Anti-de Sitter black holes, Phys. Lett. B 723(2013)436-441

[7] X. X. Zeng, X. M. Liu and L. F. Li, Phase structure of the Born-Infeld-anti-de Sitter black holes probed by non-local observables, arXiv:1601.01160

[8] E. Caceres, P. H. Nguyen and J. F. Pedraza, Holographic entanglement entropy and the extended phase structure of STU black holes, JHEP 1509 (2015) 184

[9] X. X. Zeng, H. Zhang and L. F. Li, Phase transition of holographic entanglement entropy in massive gravity, Phys. Lett. B 756(2016)170-179

[10] A. Dey, S. Mahapatra, T. Sarkar, Thermodynamics and Entanglement Entropy with Weyl Corrections, arXiv:1512.07117

[11] X. X. Zeng and L. F. Li, Van der Waals phase transition in the framework of holography, arXiv:1512.08855

[12] S. Kundu and J. F. Pedraza, Aspects of Holographic Entanglement at Finite Temperature and Chemical Potential, arXiv:1602.07353

[13] D. Momeni, K. Myrzakulov and R. Myrzakulov, Fidelity Susceptibility as Holographic P-V criticality, arXiv:1604.06909

[14] J. X. Mo, G. Q. Li, Z. T. Lin and X. X. Zeng, Van der Waals like behavior and equal area law of two point correlation function of $f(R)$ AdS black holes, arXiv:1604.08332

[15] Y. Sun, H. Xu and L. Zhao, Thermodynamics and holographic entanglement entropy for spherical black holes in 5D Gauss-Bonnet gravity, arXiv:1606.06531

[16] G. W. Gibbons and K. Maeda, Black Holes and Membranes in Higher Dimensional Theories with Dilaton Fields, Nucl. Phys. B 298(1988)741

[17] T. Koikawa and M. Yoshimura, Dilaton Fields and Event Horizon, Phys. Lett. B 189(1987)29

[18] D. Garfinkle, G. T. Horowitz and A. Strominger, Charged black holes in string theory, Phys. Rev. D 43(1991)3140

[19] R. Gregory and J. A. Harvey, Black holes with a massive dilaton, Phys. Rev. D 47(1993)2411

[20] M. Rakhmanov, Dilaton black holes with electric charge, Phys. Rev. D 50(1994)5155

[21] K. C. K. Chan, J. H. Horne and R. B. Mann, Charged dilaton black holes with unusual asymptotics, Nucl. Phys. B 447(1995)441-464

[22] R. G. Cai, J. Y. Ji and K. S. Soh, Topological dilaton black holes, Phys. Rev D 57(1998)6547

[23] R. G. Cai and Y. Z. Zhang, Holography and brane cosmology in domain wall backgrounds. Phys. Rev D 64(2001)104015

[24] G. Clement, D. Gal'tsov and C. Leygnac, Linear dilaton black holes, Phys. Rev. D 67(2003)024012

[25] G. Clement and C. Leygnac, Non-asymptotically flat, non-AdS dilaton black holes, Phys. Rev. D 70(2004)084018

[26] C. J. Gao and H. N. Zhang, Topological Black Holes in Dilaton Gravity Theory, Phys. Lett. B 612(2006)127-136

[27] S. J. Poletti and D. L. Wiltshire, The Global properties of static spherically symmetric charged dilaton space-times with a Liouville potential, Phys. Rev. D 50(1994)7260

[28] K. Goldstein, S. Kachru, S. Prakash and S. P. Trivedi, Holography of Charged Dilaton Black Holes, JHEP 1008(2010)078

[29] K. Goldstein, N. Lizuka, S. Kachru, S. Prakash, S. P. Trivedi and A. Westphal, Holography of Dyonic Dilaton Black Branes, JHEP 1010(2010)027

[30] C. M. Chen and D. W. Peng, Holography of Charged Dilaton Black Holes in General Dimensions, JHEP 1006(2010)093

[31] B. Gouteraux, B. S. Kim and R. Meyer, Charged Dilatonic Black Holes and Their Transport Properties, Fortschr. Phys. 59(2011)723

[32] S. S. Gubser, F. D. Rocha, Peculiar Properties of a Charged Dilatonic Black Hole in AdS_5, Phys. Rev. D81(2010)046001

[33] Y. C. Ong and P. Chen, Stringy Stability of Charged Dilaton Black Holes with Flat Event Horizon, JHEP 1208(2012)79

[34] W. J. Li, Some Properties of the Holographic Fermions in an Extremal Charged Dilatonic Black Holes, Phys. Rev. D84(2011)064008

[35] W. J. Li, R. Meyer and H. Zhang, Holographic Non-Relativistic Fermionic Fixed Point by the Charged Dilatonic Black Hole, JHEP 01 (2012) 153

[36] R. Zhao, H. H. Zhao, M. S. Ma and L. C. Zhang, On the critical phenomena and thermodynamics of charged topological dilaton AdS black holes, Eur. Phys. J. C73 (2013) 2645

[37] M. H. Dehghani, S. H. Hendi, A. Sheykhi and H. Rastegar Sedehi, Thermodynamics of Rotating Black Branes in Einstein–Born-Infeld-dilaton Gravity, JCAP 02(2007)020

[38] A. Sheykhi, N. Riazi, Thermodynamics of black holes in (n+1)-dimensional Einstein-Born-Infeld dilaton gravity, Phys. Rev. D75(2007)024021

[39] S. H. Hendi, A. Sheykhi and M. H. Dehghani, Thermodynamics of Higher Dimensional Topological Charged AdS Black Branes in Dilaton Gravity, Eur. Phys. J. C 70(2010)703

[40] A. Sheykhi, M. H. Dehghani, S. H. Hendi, Thermodynamic Instability of Charged Dilaton Black Holes in AdS Spaces, Phys. Rev. D 81(2010)084040

[41] A. Sheykhi and S. Hajkhalili, Dilaton black holes coupled to nonlinear electrodynamic field, Phys. Rev. D 89(2014)104019

[42] A. Sheykhi and A. Kazemi, Higher dimensional dilaton black holes in the presence of exponential nonlinear electrodynamics, Phys. Rev. D 90(2014)044028

[43] M. H. Dehghani, S. Kamrani and A. Sheykhi, P-V criticality of charged dilatonic black holes, Phys. Rev. D 90(2014)104020

[44] M. K. Zangeneh, A. Sheykhi and M. H. Dehghani, Thermodynamics of higher dimensional topological dilation black holes with a power-law Maxwell field, Phys. Rev. D 91(2015)044035

[45] M. K. Zangeneh, M. H. Dehghani and A. Sheykhi, Thermodynamics of charged rotating dilaton black branes with power-law Maxwell field, Eur. Phys. J. C75 (2015)497

[46] A. Sheykhi, F. Naeimipour and S. M. Zebarjad, Phase transition and thermodynamic geometry of topological dilaton black holes in gravitating logarithmic nonlinear electrodynamics, Phys. Rev. D 91(2015)124057

[47] A. Sheykhi, F. Naeimipour and S. M. Zebarjad, Thermodynamic geometry and thermal stability of n-dimensional dilaton black holes in the presence of logarithmic nonlinear electrodynamics, Phys. Rev. D 92(2015)124054

[48] S. H. Hendi, A. Sheykhi, S. Panahiyan and B. Eslam Panah, Phase transition and thermodynamic geometry of Einstein-Maxwell-dilaton black holes, Phys. Rev. D92 (2015)064028

[49] M. H. Dehghani, A. Sheykhi and Z.Dayyani, Critical behavior of Born-Infeld dilaton black holes, Phys.Rev. D 93(2016)024022

[50] J. X. Mo, G. Q. Li and X. B. Xu, Effects of power-law Maxwell field on the critical phenomena of higher dimensional dilaton black holes, Phys. Rev. D 93 (2016)084041

[51] V. Balasubramanian and S. F. Ross, Holographic particle detection, Phys. Rev. D 61(2000)044007

[52] S. Ryu and T. Takayanagi, Holographic derivation of entanglement entropy from AdS/CFT, Phys. Rev. Lett. 96, 181602 (2006)

[53] S. Ryu and T. Takayanagi, Aspects of Holographic Entanglement Entropy, JHEP 0608, 045 (2006)